ELSEVIER

Polymer 42 (2001) 5321–5326

polymer

www.elsevier.nl/locate/polymer

Structural transformation of polyethylene phase in oriented polyethylene/polypropylene blends: a hierarchical structure approach

P. Schmidt[a,*], J. Baldrian[a], J. Ščudla[a], J. Dybal[a], M. Raab[a], K.-J. Eichhorn[b]

[a]*Institute of Macromolecular Chemistry, Academy of Sciences of the Czech Republic, Heyrovský Sq. 2, 162 06 Prague, Czech Republic*
[b]*Institute for Polymer Research, Hohe Strasse 6, 01005 Dresden, Germany*

Received 30 August 2000; received in revised form 29 November 2000; accepted 7 December 2000

Abstract

Injection-moulded specimens of polyethylene/polypropylene blends were drawn at room temperature and subsequently annealed at 140°C, i.e. above the melting temperature of polyethylene, but below the melting temperature of isotactic polypropylene. Structural transformations of the polyethylene phase were assessed at several levels of hierarchical structure by polarised FTIR spectroscopy with photoacoustic detection, DSC, WAXS and SAXS analyses, and dynamic mechanical analysis. The results indicate reorientation of polyethylene chains, corresponding rearrangement of crystalline lamellae and healing of interfibrillar flaws upon annealing.

Keywords: Polarised FTIR spectroscopy with photoacoustic detection; X-ray diffraction; Dynamic mechanical behaviour of polyethylene/polypropylene blends

1. Introduction

Polyolefins are typical commodity polymers with many application areas and a remarkable growth rate. The reason is not only a favourable price/performance ratio, but also the versatility of these materials and a very broad range of possible modifications, which makes possible tailoring of end-use properties. Chemical modifications, copolymerisation, blending, drawing, thermal treatment and combination of these techniques can convert common-grade polyolefins to valuable products with special properties. For example, an addition of a small amount of a suitable compatibiliser was recently shown to enhance the toughness of polyethylene (PE)/polypropylene (PP) blends dramatically [1]. A composite material consisting of PP fibrils embedded in continuous PE matrix, prepared by cold drawing and subsequent annealing at fixed length, was also described [2]. Similar PE/PP systems were studied many times mostly in thinner layers [3–16]. A careful analysis of X-ray data yielded a quantitative assessment of the recrystallisation and reorientation of polyethylene chains proceeding via epitaxial growth of PE on the PP matrix [7,10,11].

For a clearer understanding of the structural transformations in the technologically relevant thick PE/PP specimens a series of structure sensitive methods was used in this study — polarised FTIR spectroscopy with photoacoustic detection (PPA FTIR), DSC, WAXS, SAXS and dynamic-mechanical analysis (DMA). In particular, PPA FTIR appeared recently as a valuable tool for the characterisation of molecular orientation in bulk material [17,18]. This modern spectroscopic method can estimate the chain orientation in thick oriented specimens and can even assess the skin–core effects.

The methods selected for this study allowed the characterisation of the structural transformations of bulk thick specimens at several levels of the hierarchical structure: orientation of the molecular chains, recrystallisation of lamellae and their stacks, and healing of flaws. Thus, the outcome of this work has direct consequences for the structure of real injection-moulded parts.

From the combination of individual results of this study a complex picture of the transformation of the whole hierarchical structure was derived.

2. Experimental

2.1. Materials and specimens

Isotactic polypropylene Mosten 58412, batch 834/93

* Corresponding author. Tel.: +420-2-20403381; fax: +420-2-35357981.
E-mail address: schmidt@imc.cas.cz (P. Schmidt).

0032-3861/01/$ - see front matter
PII: S0032-3861(00)00928-9

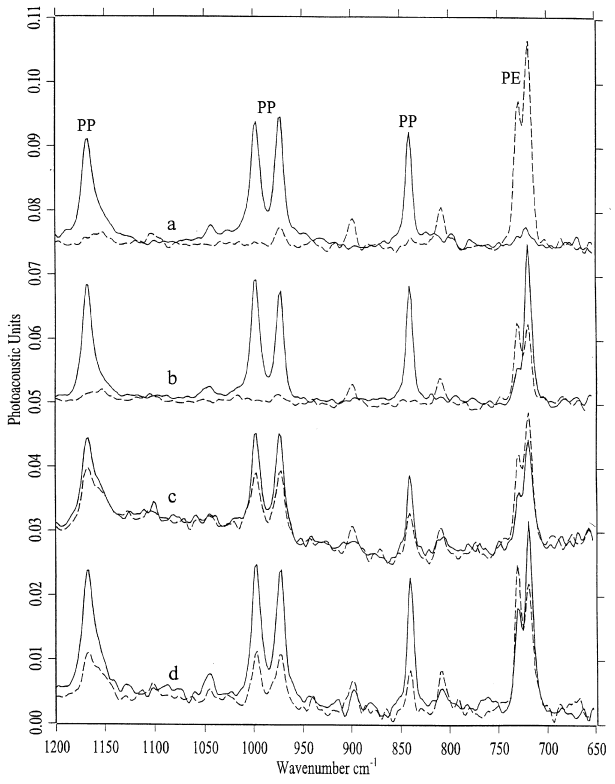

Fig. 1. Polarised PA FTIR spectra of cold-drawn specimens of 50/50 PE/PP blend: (a) before annealing, surface; (b) after annealing to 140°C, surface; (c) before annealing, inner portion; (d) after annealing to 140°C, inner portion. Electric vector — parallel, – – – perpendicular to drawing.

(PP), and high-density polyethylene Liten MB 62 (PE) were the basic materials for this study. Both polymers were supplied by Chemopetrol Litvínov, Czech Republic. The experimental model blend was prepared by mixing PP and PE pellets (mass ratio 50/50) first in a Banbury mixer and then in a double-screw extruder. Standard dumbbell test pieces were prepared by injection moulding. The processing conditions for specimen preparation were described elsewhere [19]. The gauge length, width and thickness of the injection-moulded test pieces were 90, 10, and 4 mm, respectively. The prepared test pieces were drawn at 23°C at a test speed of 20 mm min^{-1} using an Instron 6025. The drawing was heterogeneous, i.e. concentrated in a sharp neck shoulder. The obtained draw ratio reached the value of 5.1. The cold-drawn specimens were then exposed to an annealing in a vacuum oven at 140°C for 20 h and slowly cooled down. After the annealing, some shrinkage was observed which led to a resulting draw ratio of 4.6, i.e. the original draw ratio decreased by 9.8%. For the measurement of PPA FTIR spectra of the inner portion of the specimens, the drawn specimens were split along the draw direction into two halves under liquid nitrogen.

2.2. IR spectroscopy

Polarised photoacoustic Fourier-transform infrared (PPA-FTIR) measurements were performed with an infrared spectrometer Bruker IFS66v/S using an MTEC 200 photoacoustic cell (Ames, IW). Experimental and theoretical details of this technique were described in our previous papers [17,18]. For measurements of the surface regions of the material, specimens of approximate dimensions of $8 \times 4 \times 2\ mm^3$ were cut from the drawn portions of cold-drawn specimens to fit into the cell holder. To analyse the inner part, cleaved samples of approx. dimensions of $4 \times 2 \times 2\ mm^3$ were used. After inserting the cell holder with the specimen into the spectrometer, the cell was flushed with He for at least 1 h before the beginning of the measurement. The resolution was $4\ cm^{-1}$, and a carbon-black standard was used as a reference. The infrared spectra were measured with a mirror frequency of 2.2 kHz, 1000 scans being accumulated. The direction of the specimen orientation coincided with the plane in which the infrared beam passes through the photoacoustic cell. A KRS-5 wire grid polariser (SPECAC) was placed immediately in front of the cell. Two successive measurements, with parallel ($\parallel$) and with perpendicular ($\perp$) polarisation of the electric vector with respect to the draw direction of the specimen, were performed.

2.3. X-ray diffraction

WAXS measurements were performed with a flat-film camera. For SAXS measurements, a Kratky camera (A. Paar, Austria) was employed. Monochromatised CuKα radiation was used.

2.4. DMA

Rheometrics *System Four* was used for obtaining the real G' and imaginary G'' parts of the complex shear modulus of elasticity G^*. The specimens were bars cut from injection-moulded, drawn and annealed test pieces and their thermal expansion was compensated during the measurement. The specimen geometry was as follows: the distances between clamps, width, and thickness were 40, 10 and 4 mm for injection-moulded specimens, 25, ~4 and ~2 mm for drawn specimens, both before and after annealing. Torsion forced vibrations were applied to the specimen with a frequency of 1 Hz. The temperature sweep mode was used in the interval from 150°C to the melting temperature of the particular specimen (about 130–170°C). The measurements were carried out at increments of 3°C with heating rate of 1°C min^{-1}.

2.5. DSC measurements

DSC thermograms were obtained with a Perkin–Elmer Pyris 1 DSC. The heating rate was 10°C min^{-1}. The difference in the melting points of PE and PP allowed to evaluate

the melting peaks and to estimate the crystallinity values of the components separately.

The following results were obtained for injection-moulded, drawn and subsequently annealed specimens, respectively: crystallinity 42, 52 and 61%, T_m = 166–167°C, for PP; crystallinity 55, 61 and 74%, T_m = 132–134°C, for PE. (The values of 206 and 292 J/g were used as heats of fusion for 100% crystalline PP and PE, respectively [20]). A marked increase in crystallinity upon annealing, particularly for the PE component, is evident.

2.6. Densitometry

Density values of the original injection-moulded, of the subsequently drawn, and of the subsequently annealed specimens determined by weighing in methanol at room temperature were 0.918, 0.626 and 0.924 g cm^{-3}, respectively.

3. Results and discussion

3.1. Molecular and supermolecular structure

In Fig. 1a, the PPA FTIR spectra of the surface of the drawn specimen are presented. The measured intensities in the infrared photoacoustic spectroscopy are known to show strong dependence on the effective penetration depth d {$d = (\sigma/\rho C_p \pi f)^{1/2}$, where σ is the thermal conductivity, ρ the sample density, C_p the heat capacity and $f = v\nu$ the modulation frequency determined by the velocity of the mirror v and the frequency of the radiation ν} [21]. For the fixed mirror frequency of 2.2 kHz used in our measurements it means that for the different wavelengths the probing depths are different. However, this fact influences neither the infrared dichroisms of the bands measured at fixed wavelengths nor the relative comparison of the 720 and 730 cm^{-1} PE bands having nearly identical probing depths.

As follows from the measured infrared dichroism of the characteristic PP bands with parallel dipole transition moments (e.g. 1168, 998, 973 cm^{-1} [22]) and from the measured dichroism of the characteristic PE bands with perpendicular dipole transition moments (730, 720 cm^{-1} [23,24]), both the PP and PE components of the drawn specimens exhibit a strong parallel orientation of chains with respect to the direction of drawing. The curves a in Fig. 1 suggest that about 90% of both PP and PE chains are fully oriented. In the same figure (curves b), the effect of annealing at 140°C is presented. It can be seen that the infrared dichroism of the PP bands has not changed on annealing. This is in accordance with the expectation that PP crystallites remain virtually unchanged after treatment below their melting point. Surprisingly, the characteristic bands of PE exhibit infrared dichroism as well despite the fact that polyethylene crystals melted at the annealing temperature. However, while the dichroism of the 730 cm^{-1} band changed only slightly, the dichroism of the 720 cm^{-1} band changed dramatically from perpendicular to parallel. Of the characteristic bands of PE, the 730 cm^{-1} band is assigned to the CH_2 rocking vibration of the crystalline phase and the 720 cm^{-1} band to the CH_2 rocking vibration both of the crystalline and amorphous phases [25]. It can be expected that relative intensities of the bands at 730 and 720 cm^{-1} are slightly changed upon annealing due to the increase in PE crystallinity (from 61 to 74% as determined by DSC, see above); nevertheless this effect will not significantly contribute to the observed overall large changes of band dichroisms. Therefore, we may conclude that upon annealing in the presence of the oriented PP crystallites, the PE chains were reoriented.

The curves c and d in Fig. 1 represent analogous spectra obtained for the inner parts of the drawn specimens, and of the drawn and subsequently annealed specimens, respectively. A comparison with the curves a and b shows that both before and after annealing, the orientation of the inner part of the test piece is lower than at the surface. Nevertheless, the reorientation of PE chains upon annealing shows basically the same features across the thickness of the specimen.

The results of WAXS measurements are shown in Fig. 2. The WAXS pattern of the blend after plastic deformation shows the (110), (040) and (130) reflections of PP and the (110) and (200) reflections of PE on the equator (Fig. 2a). This pattern represents a superposition of typical fibre textures of the two polymers with the chain axes oriented parallel to the draw direction. Small azimuthal widths of the reflections correspond to a highly oriented system.

However, when the drawn sample was annealed at 140°C, the orientation of PE crystallites appreciably changed, while the orientation of the c-axis (chain axis) of PP remained unchanged (Fig. 2b). In the diffraction pattern of the blend after annealing, the (200) reflection of PE remains on the equator as before, but the (020) reflection changed its position from the equator to the meridian and the (110) reflection is located at an angle of about 40° to the meridian. From these facts it follows that during annealing, the crystallographic axis a of PE crystallites did not change its perpendicular orientation with respect to drawing, whereas the axis b is now oriented in the direction of drawing. From the parameters of a PE unit cell the angle between a normal to the 110 planes and the draw direction could be estimated. The calculated value of about 34° corresponds well to the azimuthal position of the (110) reflection. In other words, after annealing, the PE chains are oriented perpendicularly to the draw direction. At the same time the broad azimuthal profiles of PE reflections demonstrate a low level of preferred orientation of the PE component after annealing. This low orientation is well demonstrated on the fibre diagram (Fig. 2b), where the (110) reflection has relatively high intensity in all directions.

The SAXS curves of the annealed specimen were measured in the directions of the equator, meridian and at the azimuth of 45° (Fig. 3). The positions of individual

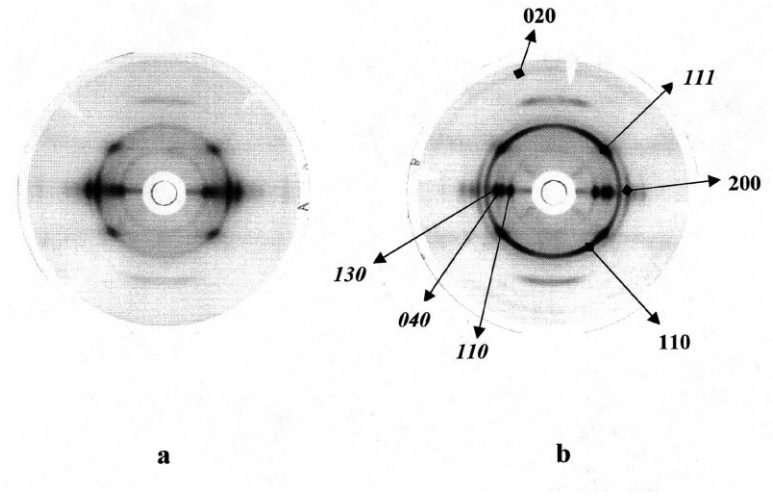

Fig. 2. Wide-angle diffraction patterns of cold-drawn specimens of 50/50 PE/PP blend: (a) before annealing; (b) after annealing to 140°C. PE, (normal script, hkl); PP, (italics, *hkl*).

peaks correspond to the lamellar periodicity (long period) in the stacks of crystallites of the particular component. The scattering curves exhibit two orders of SAXS reflection on the meridian and three orders on the equator. Such scattering curves correspond to very well developed lamellar structures and represent the main directions in which the lamellar stacks in annealed sample are oriented. Based on the WAXS results, the lamellar stacks with periodicity of 23 nm oriented in the draw direction (meridian) correspond to the PP component and the lamellar stacks with periodicity of 39 nm oriented in the direction of equator correspond to the PE component. The appearance of the reflection on the SAXS scattering curve in the direction tilted by 45° to the meridian (corresponding to the PE lamellar stacks with periodicity of about 40 nm) suggests a low orientation of the PE component. The intensity of this reflection in 45° direction is lower by about 30% then in the direction of the equator and is much broader. From this observation it follows that only a small fraction of the lamellar stacks of PE is oriented in this direction and that their structure is considerably less developed.

As the polymer chains of both PP and PE are oriented perpendicularly to the lamellar surfaces, i.e. parallel to the lamellar stacks, it follows that after annealing, the chains of PP remain oriented in the draw direction whilst the PE chains are oriented perpendicularly to it. Obviously, these results are in agreement with the PPA FTIR data on the orientation of individual chains.

Series of works [3–16] were devoted to the reorientation of PE component during recrystallisation in highly oriented PP/PE blends. Lotz and Wittmann [7,10] suggested an epitaxial growth during the annealing of oriented PE/PP blends. The characteristic feature of such model is ~50° mutual tilting of PP and PE chain axes. The same authors have shown that this interpretation holds also for other observations in this field [11]. Our results of PPA FTIR, WAXS and SAXS suggest a different model of this structural reorientation. We have shown that after annealing of our system the PP and PE chain axes are mutually perpendicular. Besides, the comparisons of our fibre diagram (Fig. 2b) with the diagrams published earlier [3–16] suggests much lower orientation of the PE component in the present case. The relatively high amount (50 wt.%) of the PE component, thicker oriented specimens annealed with free ends and larger PE microdomains (~1–2 μm) [26] are probably the reasons of these differences. An epitaxial growth of PE lamellae, if it does exist in our case at all, would be limited to a very narrow layer at the interface between the PP and PE phases. In a larger distance from

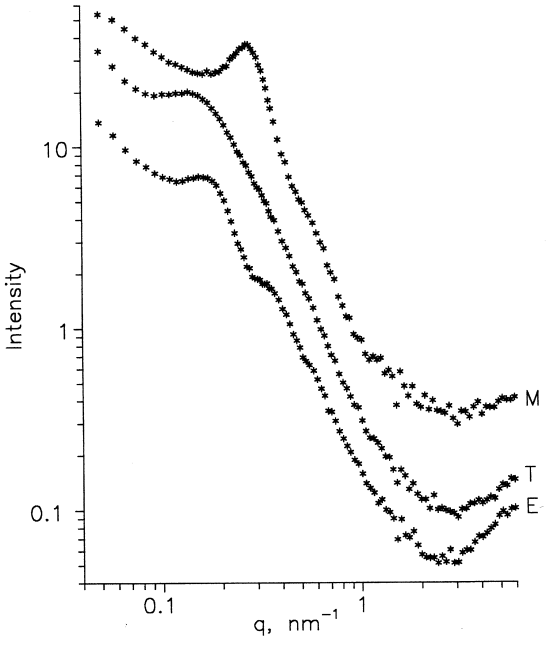

Fig. 3. SAXS measurement of cold-drawn specimen of 50/50 PE/PP blend after annealing to 140°C. Curves measured in the direction of meridian (M), of equator (E) and tilted 45° from meridian (T).

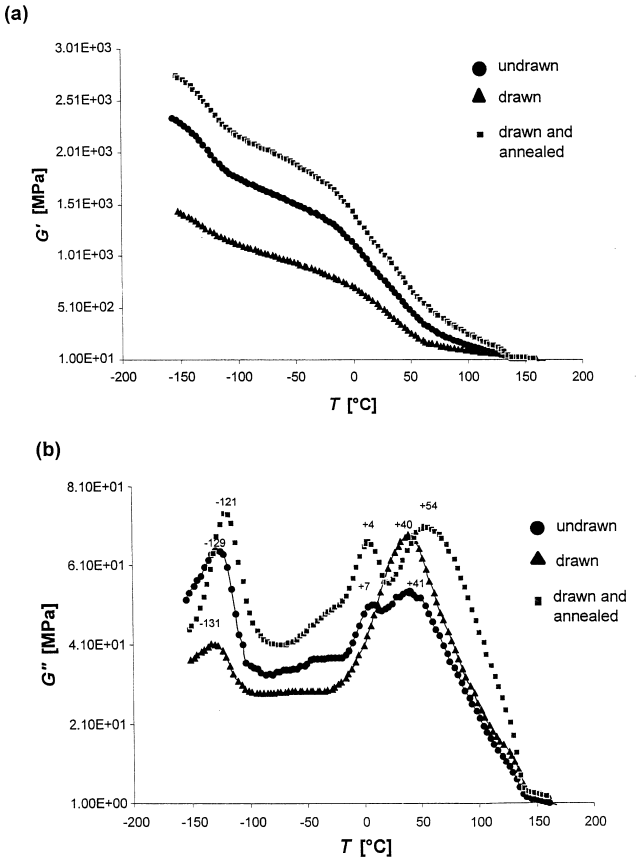

Fig. 4. Temperature dependencies of: (a) the real G' and (b) imaginary G'' parts of the complex shear modulus of elasticity G^* for injection-moulded (undrawn), for cold-drawn and for subsequently annealed specimens.

the interface the epitaxial orientation is definitively lost and the lamellae grow in the direction of the largest dimension of the PE regions.

PPA FTIR measurements made by step-by-step turning of the polariser have shown extreme values of dichroism for the 730 and 720 cm^{-1} bands at the positions of 0° and 90°. The bands at 730 and 720 cm^{-1} belong to symmetry species B_{1u} and B_{2u}, respectively. The first band is polarised along the *a*-axis, whereas the second band along the *b*-axis of the crystal [25]. For axial orientation, a model of preferred reorientation of the PE chains in the drawn PE/PP blend after annealing can be formulated, in accordance with the X-ray results. In this model, the PE crystallites previously oriented with the *c*-axis (chain direction) parallel to the drawing are reoriented so that the *c* and *a* axes are now perpendicular to the direction of the plastic deformation, whereas the *b*-axis is parallel to it. It is worth noting that the originally better orientation of PE molecules in the skin layer of the drawn specimens led also to more perfect reorientation in the skin after annealing, as compared to the inner core of the specimen (see Fig. 1). It is possible that the skin and core layers of the oriented specimens differ not only in the chain orientation but also in crystallinity. Nevertheless, this possible crystallinity difference cannot basically change our conclusions.

Mencik et al. [27] have reported that the crystal growth of PE lamellae in oriented blends proceeds preferentially along the draw direction. For melt-spun PE/PS blend fibres, they concluded that the PE lamellae grow preferentially with *b*-axis parallel to the draw direction, as the fastest growth of the PE crystals proceeds preferentially along the longer dimension of the confined space. Obviously, our results of PPA FTIR spectra and X-ray diffraction can be explained by a similar preferential growth of PE lamellae along and between the oriented PP fibrils in the elongated needle-like spaces left after melting of the PE fibrils rather than by an epitaxial growth. Consequently, after annealing, the PE chains in these lamellae are oriented perpendicularly to the draw direction.

3.2. Dynamic mechanical properties

The significant morphological changes associated with cold drawing and subsequent annealing are also manifested by dynamic mechanical behaviour. The temperature dependencies of the real part G' (storage modulus) and the imaginary part G'' (loss modulus) of the complex shear modulus of elasticity G^* for injection moulded (undrawn), for drawn and for subsequently annealed specimens are shown in Fig. 4a and b. The dependencies of the storage modulus (Fig. 4a) with marked decrease at the T_g of the amorphous phase of PP show the dominating role of the PP component in the elastic behaviour of the blend. Three characteristic maxima of the loss modulus (Fig. 4b) could be ascribed to the motion of short segments of the PE chain (−129°C), glass transition temperature T_g of the PP (+7°C) and melting of crystallites of both the PE and PP components (+41°C). (Slight shifts of these loss maxima as compared to dynamic *tensile* data published earlier [28] could be ascribed to different experimental conditions.)

From the comparison of the dynamic mechanical behaviour of the three samples under study the following structural conclusions can be drawn. (1) The decrease of the low-temperature loss maximum upon drawing followed by a marked increase after annealing indicates formation of molecular orientation of the PE component accompanied by lower molecular mobility and subsequent reorientation accompanied by overall increase of material stiffness. (2) The increase of the high-temperature maximum and its shift towards higher temperatures upon drawing and subsequent annealing reflects an increase of crystallinity and an improvement of the crystalline order of both PP and PE components. This is in agreement with DSC data. (3) It seems likely that the marked decrease of the storage modulus in the whole temperature range, decrease of the loss modulus in the temperature range below 0°C and complete disappearance of the loss maximum at +7°C (T_g of PP) upon drawing reflect the formation of longitudinal flaws between oriented fibrils (structural dewetting). Indeed, elongated crazes prevent transfer of mechanical energy from stiff fibrils to soft interfibrillar regions. Consequently, the

corresponding loss maximum cannot be pronounced. After annealing, the loss maximum corresponding to the T_g of the amorphous PP reappears and is even more pronounced than with the injection-moulded undrawn polymer. The improved compactness of the material is also indicated by a marked increase of the storage modulus in the whole temperature range. Such model based on the formation and subsequent healing of voids is supported by density measurements giving the values of 0.918, 0.626 and 0.924 g cm^{-3} for injection-moulded, drawn, and annealed materials, respectively. Visual inspection has shown that after the annealing the opaque oriented specimens have become translucent and even transparent in the skin layer.

Obviously, after annealing, PE lamellae aligned along the draw direction are formed not only in the spaces left by molten PE fibrils but also in the elongated open crazes within the cold-drawn material. The DMA results suggest not only additional crystallisation and recrystallisation but also formation of microscopic voids during cold drawing and their healing during subsequent annealing. Thus, with the polymer blend system studied, it could be demonstrated that controlled transformations of molecular orientation and crystallinity are an interesting efficient way to adjusting macroscopic mechanical properties.

4. Conclusions

1. The combination of five structure-sensitive methods (PPA FTIR, WAXS, SAXS, DSC, DMA) together with densitometry is suitable to assess structural changes during cold drawing and annealing of PP/PE blends at four structural levels (molecular orientation, crystalline structure, long period, microvoids).
2. Cold-drawn specimens show molecular orientation along the draw direction with chains and stacks of lamellae aligned parallel both for the PP and PE component. The orientation is more pronounced in the surface skin of the material than in the inner core.
3. Annealing at 140°C of the cold-drawn specimens leaves the molecular orientation of PP virtually unchanged, whereas the PE chains and stacks of lamellae of annealed specimens become oriented perpendicularly to the draw direction. Again, the resulting orientation is more perfect in the surface skin than in the inner core.
4. Overall crystallinity increases during annealing both for the PP and for the PE component.
5. DMA results support these conclusions and besides reflect formation and healing of microvoids during cold drawing and subsequent annealing. The structural transformations, improved crystalline order and compactness of both the PE and PP components after annealing, are manifested by a marked increase in the storage modulus.

Acknowledgements

We are indebted to Slovnaft Corporation, Centre of Polyolefins, Bratislava, Slovak Republic for technical support in the preparation of the model blend. Thanks are also given to Dr J. Kratochvíl of the Institute of Macromolecular Chemistry, AS CR, Prague for DSC measurements and to Mrs G. Adam, IPF Dresden, for very helpful technical assistance. Financial support of the Grant Agency of the Czech Republic and the Grant Agency of the Academy of Sciences of the Czech Republic (projects 106/97/1071, 106/98/0718, 203/97/0539, 106/99/0557 and A4050904) is gratefully acknowledged.

References

[1] Niebergall U, Bohse J, Seidler S, Grellmann W, Shürmann BL. Polym Eng Sci 1999;39:1109.
[2] Sherman ES. J Mater Sci 1984;19:4014 (and references therein).
[3] Lovinger AJ, Williams ML. J Appl Polym Sci 1980;25:1703.
[4] Nishio Y, Yamane T, Takahashi T. J Macromol Sci Phys 1984;B23:17.
[5] Kojima M, Satake H. J Polym Sci, Polym Phys Ed 1984;22:285.
[6] Gross B, Petermann J. J Mater Sci 1984;19:105.
[7] Lotz B, Wittmann JC. Makromol Chem 1984;185:2043.
[8] Hwa Lee I, Schultz JM. Bull Am Phys Soc 1985;30:444.
[9] Broza G, Rieck U, Kawaguchi A, Petermann G. J Polym Sci, Polym Phys Ed 1985;23:2623.
[10] Lotz B, Wittmann JC. J Polym Sci Polym Phys 1986;24:1559.
[11] Lotz B, Wittmann JC. J Polym Sci B, Polym Phys 1987;25:1079.
[12] Wittmann JC, Lotz B. Prog Polym Sci 1990;15:909.
[13] Petermann J, Xu Y, Loos J, Yang D. Makromol Chem 1992;193:611.
[14] Shouke Y, Lin J, Yang D, Petermann J. Macromol Chem Phys 1994;195:195.
[15] Shouke Y, Yang D, Petermann J. Polymer 1998;39:4569.
[16] Shouke Y, Katzenberg F, Petermann J. J Polym Sci, Part B: Polym Phys 1999;37:1893.
[17] Schmidt P, Raab M, Kolařík J, Eichhorn KJ. Polym Test 2000;19:205.
[18] Eichhorn KJ, Hopfe I, Pőtschke P, Schmidt P. J Appl Polym Sci 2000;75:1194.
[19] Raab M, Kotek J, Baldrian J, Grellmann W. J Appl Polym Sci 1998;69:2255.
[20] Van Krevelen DW. Properties of polymers. Amsterdam: Elsevier, 1990.
[21] Blank RE, Wakefield T. Anal Chem 1979;51:50.
[22] Miyazawa T. J Polym Sci C 1964;7:59.
[23] Elliot A, Ambrose EJ, Temple RB. J Chem Phys 1948;16:877.
[24] Tasumi M, Shimanouchi T. J Chem Phys 1965;43:1245.
[25] Stein RS, Sutherland GBMM. J Chem Phys 1954;22:1993.
[26] Schmidt P, Raab M, Quintana SL, Pastor JM. In preparation.
[27] Mencik Z, Plummer HK, Van Oene H. J Polym Sci Part A-2 1972;10:507.
[28] Amash A, Zugenmaier P. J Polym Sci Part B: Polym Phys 1997;35:1439.